IOPscience iopscience.iop.org

Home Search Collections Journals About Contact us My IOPscience

Band structure and electronic properties of the incommensurate misfit compound $(LaS)_{1.18}VS_2$

This article has been downloaded from IOPscience. Please scroll down to see the full text article.

1999 J. Phys.: Condens. Matter 11 2887

(http://iopscience.iop.org/0953-8984/11/14/005)

View the table of contents for this issue, or go to the journal homepage for more

Download details:
IP Address: 171.66.16.214
The article was downloaded on 15/05/2010 at 07:17

Please note that terms and conditions apply.

J. Phys.: Condens. Matter **11** (1999) 2887–2900. Printed in the UK PII: S0953-8984(99)00007-7

Band structure and electronic properties of the incommensurate misfit compound $(LaS)_{1.18}VS_2$

L Cario†, J Rouxel†, A Meerschaut†, Y Moelo†, B Corraze‡ and O Chauvet‡

† Laboratoire de Chimie des Solides, Institut des Materiaux de Nantes, 2 rue de la Houssiniere, BP 32229, 44322 Nantes Cédex 3, France

‡ Laboratoire de Physique Cristalline, Institut des Materiaux de Nantes, 2 rue de la Houssiniere, BP 32229, 44322 Nantes Cédex 3, France

Received 8 December 1998

Abstract. The electronic properties of the incommensurate misfit compound $(LaS)_{1.18}VS_2$ are investigated by different methods. Linear muffin-tin orbital atomic-sphere approximation band-structure calculation shows that this material should be a metal with a Fermi level located near a minimum of the density of states. Experimentally, the electrical resistivity is hopping-like while the magnetic susceptibility is metallic-like with a strong enhancement. We suggest that these paradoxical properties can be reconciled by taking into account the effects of incommensurability and electronic correlations. A comparison with commensurate $LiVS_2$ and with Ti or Cr incommensurate misfit derivatives is discussed.

1. Introduction

The misfit layered compounds $(LnX)_{1+x}TX_2$, abbreviated as '$LnTX_3$' in the following (Ln = rare earth; T = Ti, V, Cr; X = S, Se; $1.08 < 1 + x < 1.28$) have a composite structure which results from a regular alternation of LnX (rock-salt-type structure) and TX_2 (CdI_2-type structure) layers stacked along the *c*-direction (for reviews, see [1,2]). These materials exhibit a typical 2D structure with a lattice mismatch (incommensurability) occurring along one of the in-plane axes (in the *a*-direction). In these compounds, interesting physical properties related to the effects of low dimensionality and incommensurability are observed. For example the incommensurability in '$LaCrS_3$' induces a modulation of the Cr sites which is responsible for the spin-glass behaviour of this material [3].

From an electronic point of view, the misfit layered structure is stabilized via an electron transfer from the LnX slab to the TX_2 slab [2, 4]. This transfer results in a 3d band of the transition element being incompletely filled. A 2D metallic character is thus expected for these compounds, at least for T = Ti, V or Cr. In fact, it seems that the electronic properties are extremely sensitive to the nature of the transition metal in the T = Ti, V or Cr series: for instance '$CeTiS_3$' is a metal [5] while '$LaCrS_3$' is an insulator [6]. This sensitivity to the nature of the transition metal deserves some study.

For this purpose, the vanadium compounds '$LnVS_3$' between the Ti and Cr derivatives are expected to be of particular interest. '$LaVS_3$' exhibits a non-metallic resistivity [7] while the magnetic susceptibility seems to be temperature independent (metallic-like) [8]. This behaviour is imperfectly understood. Moreover, it is in contrast with that of the parent compound $LiVS_2$, where a similar charge transfer of one electron from Li to the VS_2 slab leads to a more conventional behaviour: a metallic-like resistivity and a metallic-like susceptibility.

0953-8984/99/142887+14$19.50 © 1999 IOP Publishing Ltd

In this paper we propose to clarify the origin of these physical properties and their differences. We have investigated the $(LaS)_{1.18}VS_2$ compound from two points of view. First physical measurements were carried out on well defined crystals: the same paradoxical properties are found. Then *ab initio* band-structure calculations on '$LaVS_3$' were performed. A comparison with the band structure of $LiVS_2$ is given in order to clarify the points in common for and the differences between the two compounds. We suggest that the modulation of the V sites, the electronic correlations and the position of the Fermi level in a pseudo-gap are responsible for the unconventional properties of '$LaVS_3$'. The differences from the cases of $LiVS_2$ and the Ti and Cr compounds are discussed.

Table 1. Chemical analyses of crystals from batches 1, 2 and 3 from the microprobe analyses. (*n* is the number of measurements on a single crystal.)

	Atomic per cent		
Crystal (*n*)	La	V	S
	Batch 1		
1(8)	22.18	18.85	58.97
2(3)	21.96	19.02	59.02
3(10)	22.23	18.73	59.04
4(9)	22.33	18.79	58.88
5(5)	22.21	18.77	59.02
6(5)	22.06	18.98	58.96
7(7)	22.08	18.75	59.17
Mean(47)	22.18(3)	18.82(2)	59.00(3)
Formula	$La_{1.195(2)}V_{1.014(2)}S_{3.180}$		
	Batch 1: cleaved		
1(10)	22.04(4)	18.65(4)	59.31(5)
Formula	$La_{1.182(2)}V_{1.000(2)}S_{3.180}$		
	Batch 2		
1(4)	21.63	19.12	59.25
2(7)	21.67	18.89	59.00
3(6)	21.70	19.09	59.21
4(7)	21.62	18.99	59.40
Mean(24)	21.65(4)	19.00(4)	59.31(5)
Formula	$La_{1.160(3)}V_{1.018(3)}S_{3.180}$		
	Batch 3		
1(4)	22.06	18.69	59.25
2(7)	21.97	18.93	59.10
3(6)	22.13	18.87	59.00
4(7)	21.88	19.04	59.08
Mean(24)	22.02(3)	18.87(2)	59.11(3)
Formula	$La_{1.184(3)}V_{1.015(3)}S_{3.180}$		

2. Composition and structure

The nominal composition of these materials is $(LaS)_{1.18}VS_2$. A key factor in these systems is the eventual non-stoichiometry of the material, since it can significantly modify the charge transfer. We have prepared three different batches of '$LaVS_3$' with different stoichiometries in order to set up this point. Batch 1 was prepared from a mixture of oxides heated at 1300 °C under a gas flow of H_2S for six hours. Batches 2 and 3 were obtained with an increasing excess of sulphur. For all syntheses a small amount of iodine was introduced to favour crystallization.

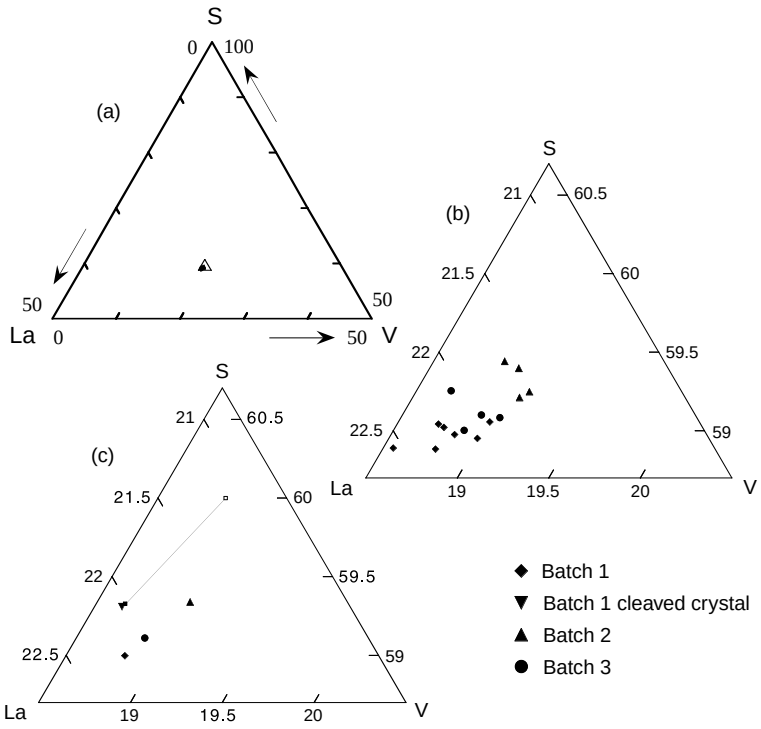

Figure 1. Projections of microprobe analyses for the three batches in the La–V–S ternary diagram (atomic percentages): (a) restricted to the part where [S] > 50%; (b) enlarged around the monolayer data (58 < [S] < 63%); (c) enlarged around the mean analyses of the three batches. The solid line in figure 1(c) is the limit between the vacancy-rich and the non-vacancy poles.

The precise composition of our materials was determined by electron microprobe analysis performed at the BRGM-CNRS laboratory (Orleans, France). Several crystals from each batch were analysed. The quality of the crystals was checked optically before the analysis. The results and operating conditions are given in table 1. For all samples, the iodine content is very low and will be neglected hereafter. The La–V–S ternary diagram (atomic percentages) as deduced from this analysis is shown on figure 1. Figure 1(a) is restricted to [S] > 50 at.%. Zooms around the monolayer composition (58% < [S] < 63%) are given in figure 1(b) and

figure 1(c). It is clear from figure 1(b) that the crystals from batches 1 and 3 are less rich in S and V poorer than those from batch 2. This is confirmed by figure 1(c) where we have only plotted the average composition for each batch: the highest sulphur content is found for batch 2.

We have also analysed the composition of a freshly cleaved surface of a millimetre-size lamella from batch 1 without any polishing. The analysis gives almost the same La/V cationic ratio as for the polished samples of the same batch but with a significantly higher S content (figure 1(b)). This difference is due to the surface oxidation of the polished samples [9]. Taking into account this systematic shift together with the experimental uncertainties, the solid solution revealed by electron microprobe analysis agrees with a general formula $(La_{1-x}S)_{1.18}VS_2$. Samples from batch 1 are stoichiometric with $x \sim 0$; i.e. the LaS layer is vacancy free. On the other hand, batch 2 is vacancy rich with $x \sim 0.04$. Note that this vacancy content does not reach the theoretical maximum of 0.06 (=1/3 of 0.18) predicted by Rouxel *et al* [10] for $(GdS)_{1.27}CrS_2$ and other Ln/Cr misfits. However, x-values higher than 0.04 might also occur in '$LaVS_3$' compounds.

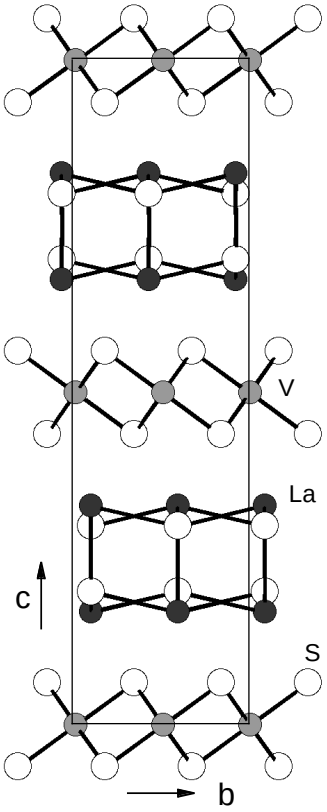

Figure 2. The projection of the structure of '$LaVS_3$' onto the (b, c) plane.

These different contents of La vacancies in the LaS layers explain the slight differences observed among the lattice parameters of the three different batches. The structure of '$LaVS_3$' has been determined by Kato *et al* [11]. It consists of a regular stacking of LaS and VS_2 layers (cf. figure 2). The two subsystems formed a C-centred orthorhombic lattice with unit-cell parameters $a_{VS_2} = 3.366$ Å, $a_{LaS} = 5.705$ Å, $b = 5.828$ Å and c close to 22.32 Å. The b-

and c-parameters are common to the two substructures while the a-vectors are parallel, with an incommensurate length ratio $a_{VS_2}/a_{LaS} = 0.590$ close to 5/3. The LaS part adopts a NaCl distorted structure type, while in the VS_2 slab, V atoms are each octahedrally surrounded by six S atoms. In our samples, x-ray diffraction gives the following parameters of the LaS subsystem. In batch 1, $a = 5.722(2)$ Å, $b = 5.818(2)$ Å and $c = 22.21(1)$ Å, while in batch 2, $a = 5.700(6)$ Å, $b = 5.814(2)$ Å and $c = 22.36(2)$ Å. These parameters are comparable to Kato's results. The significant increase of the c-parameter (+0.15 Å) is related to the sulphur excess in batch 2 as shown by Kikkawa *et al* [12]. It is in agreement with our chemical analysis discussed above. Our highest c-value is close to the maximum of 22.37 Å reported in reference [12] (highest sulphur content) while our lowest value is just above their minimum value (22.175 Å).

Starting from a vacancy-free monolayer, a vacancy-rich derivative can be obtained with increasing sulphur fugacity up to the ideal limit where all of the cations are in trivalent states. Our data are in agreement with the model of a variable Ln vacancy level previously proposed for the misfit compound $(SmS)_{1.25}TiS_2$ [13]. This means that a solid solution of nominal composition $(La_{1-x}S)_{1.18}VS_2$ exists in this family also. Indeed, a precise knowledge of the chemical composition is required in order to discuss the electronic properties of these materials. In the remainder of this study, we will focus on samples from batch 1 which are stoichiometric ($x \sim 0$).

3. Band structure and stability

The stability of '$LaVS_3$' is due to the strong charge transfer from the donor part LaS to the acceptor part VS_2 (note that the binary compound VS_2 is very unstable). Ideally up to $1 + x$ electrons per V atom could be transferred from the LaS part to the VS_2 one. Whatever the transfer, the V t_{2g} band should be incompletely filled. A metallic conduction is thus expected for '$LaVS_3$' as well as in the misfit compounds with T = Ti or Cr. We have already noticed that only Ti compounds show clearly a metallic character. Recent band-structure calculations succeeded in explaining the insulating behaviour of the Cr compounds '$LnCrS_3$' and their non-stoichiometry [6]. The calculations have shown that the t_{2g} bands of Cr are spin polarized and that a gap opens between the $t_{2g}(\uparrow)$ and the $t_{2g}(\downarrow)$ bands. This gap prevents a charge transfer of more than one electron per Cr atom. For this reason, the ideal compound of nominal composition $(LaS)_{1.20}CrS_2$ is not stable since this composition would lead to a transfer of 1.2 electrons/Cr. In fact, the stable composition is $(La_{0.94}S)_{1.20}CrS_2$ for which exactly 1 electron/Cr is transferred: the material thus behaves like a Mott insulator [6]. This non-stoichiometry is due to the formation of 6% La vacancies in the LaS slab. This has been confirmed by an accurate chemical analysis [10].

We tried to adopt the same approach for $(LaS)_{1.18}VS_2$, i.e. to perform a band-structure calculation. To do this, we approximated the incommensurate structure by the nearest commensurate superstructure (according to the vernier rule). We used the simplest commensurate cell, which is built from five unit cells of VS_2 and exactly three (rather than 2.95) unit cells of LaS along the a-direction, the b- and c-parameters remaining unchanged. The new a-periodicity is chosen exactly equal to five times that of VS_2 since this part is more rigid than the LaS part. This means that in our calculation the VS_2 part is not altered while the LaS slab is slightly contracted along the a-direction. The differences in the interatomic distances induced by this slight contraction are extremely small: we assume that they will not drastically affect the main results of our calculation. The symmetry of this structure is $C1$. Since $C1$ is not a conventional space group, we used the unit cell sketched in figure 3 with symmetry $P1$. The formula unit is $La_{12}V_{10}S_{32}$. The lattice parameters are: $a_p = 8.905$ Å,

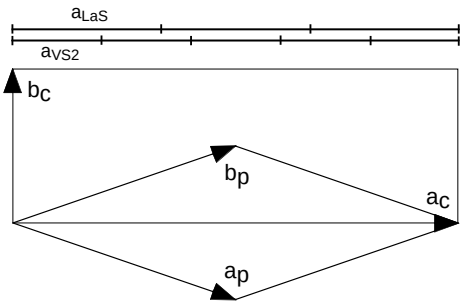

Figure 3. The relationship between the unit cell used for band-structure calculations ($P1$), and for commensurate structure description ($C1$).

$b_p = 8.905$ Å, $c = 22.32$ Å, $\alpha = \beta = 90^\circ$, $\gamma = 38.2^\circ$.

A self-consistent, *ab initio*, band-structure calculation was performed using the tight-binding representation of the LMTO-ASA method (the TB-LMTO-ASA47 program [14]). The usual criterion of a totally filled crystal volume was met by introducing 47 interstitial spheres (0.91 Å $< R_{ES} <$ 1.22 Å). For any couple of atom-centred spheres the radial overlap did not exceed 15%. This means that the conditions for accurate calculations are reached. The Wigner–Seitz atomic-sphere radii, and the positions and the radii of the empty spheres have been determined by an automatic procedure [15]. The atomic partial waves used in the calculations were 6s, 6p, 5d and 4f for La, 4s, 4p, 3d for V atoms and 3s, 3p, 3d for S, respectively. The La 6p and the S 3d states were not directly included in the basis set but treated by the down-folding technique [15]. 54 k-vectors of the first Brillouin zone were used to obtain a slow, smooth convergence of the self-consistency process.

It should be noticed that our computer cannot handle spin-polarized conditions on the whole $La_{12}V_{10}S_{32}$ cell. However, because this point is of importance, such a calculation has been performed on the VS_2 part of the structure. It shows that the V t_{2g} band is weakly polarized if it is, in sharp contrast with the case of Cr compounds. This is in agreement with our magnetic measurements on '$LaVS_3$', which show that the vanadium atoms are non-magnetic. In the following the calculations will be performed without spin polarization.

The total density of states and the partial DOS of the V 3d atoms, the LaS layer and the VS_2 layer are shown in figures 4(a), 4(c), 4(b) and 4d respectively. The Fermi level is located at the origin of the energy scale. The total DOS shown in figure 4(a) can be described as follows. The lowest band (at around -13.5 eV) consists mainly of S 3s orbitals. In fact, S from VS_2 contributes mainly at the bottom of this band (figure 4(d)) while the top comes from the LaS slab (figure 4(b)). This separation in energy reflects the fact that the La–S bonds are more ionic than the V–S bonds. S 3p bands are found in the $[-7, -1.3]$ eV region. They are hybridized weakly with the La 5d orbitals, and more strongly with the V 3d states. Here again the S 3p states of the VS_2 layer are found in the lower part of the band while those of the LaS slab are in the upper part. However, a small admixture of S 3p and La 5d contributions from LaS in the lower part of this S 3p band indicates weak interlayer interactions. Around the Fermi level, from -1.3 to 3 eV, the V 3d orbitals mixed with S 3p ones are found (figure 4(b)). This band is split into a t_{2g} band and an e_g band as is usual for transition elements in an octahedral environment. The t_{2g} band is dispersed over more than 2.3 eV: this suggests a rather strong overlap. It is filled with 2.2 electrons per V atom. The calculation does not give any band dominated by the La states below the Fermi level. The La 5d states are located just above the Fermi level while the La 4f bands are found 3 eV above. This means that the La atoms are

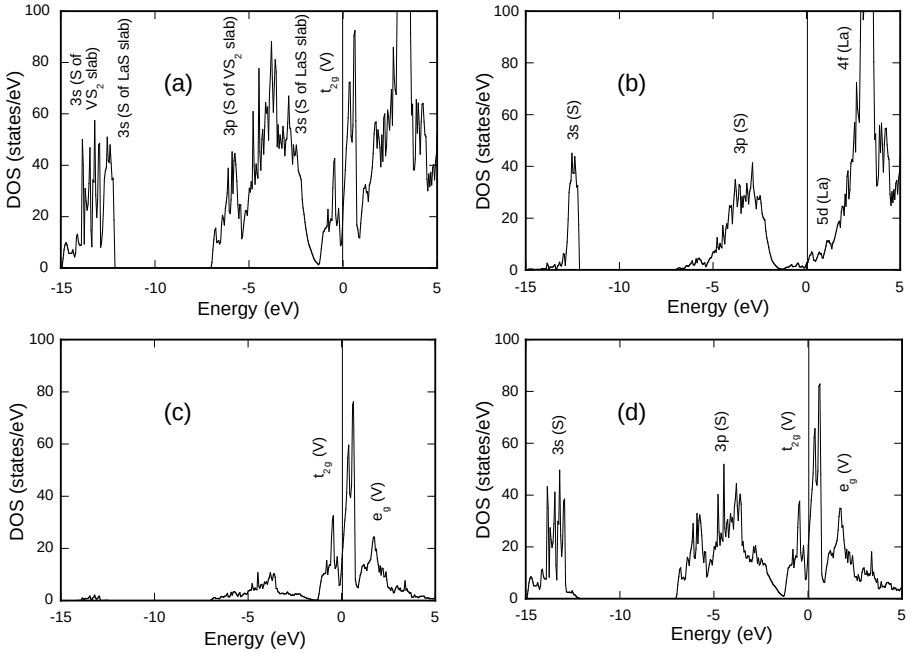

Figure 4. The density of states (DOS) of '$LaVS_3$' (formula unit $La_{12}V_{10}S_{32}$). (a) The total density of states. (b) The partial DOS of LaS layers. (c) The projected DOS of the V 3d orbitals. (d) The partial DOS of VS_2 layers.

completely ionized to the +3 state, which shows that the charge transfer is complete.

Band structures of hypothetically isolated LaS and VS_2 layers have also been calculated within the geometry of the misfit compound. Compared to the partial DOS shown in figures 4(b) and 4(d), the main difference is the shift of the LaS part towards higher energies when the two layers are interacting. This shift is a consequence of the charge transfer from the LaS slab to the VS_2 layer in the '$LaVS_3$' compound. In fact this calculation shows that the band structure of '$LaVS_3$' can be regarded as a superposition of the rigid bands of each separate slab stabilized by the charge transfer. As already shown for '$LaCrS_3$' [6] it suggests also that the cohesion of the layers in '$LaVS_3$' is due to the ionic interactions resulting from this charge transfer.

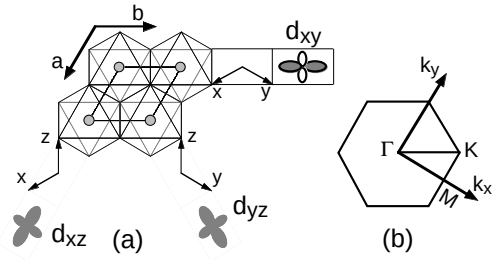

Figure 5. (a) The ideal octahedral TX_2 layer due to edge-sharing octahedral chains running along the direction $\boldsymbol{a}$, $\boldsymbol{b}$ or $\boldsymbol{a} + \boldsymbol{b}$. (b) The first Brillouin zone for the hexagonal lattice corresponding to the symmetry of the octahedral TX_2 layer.

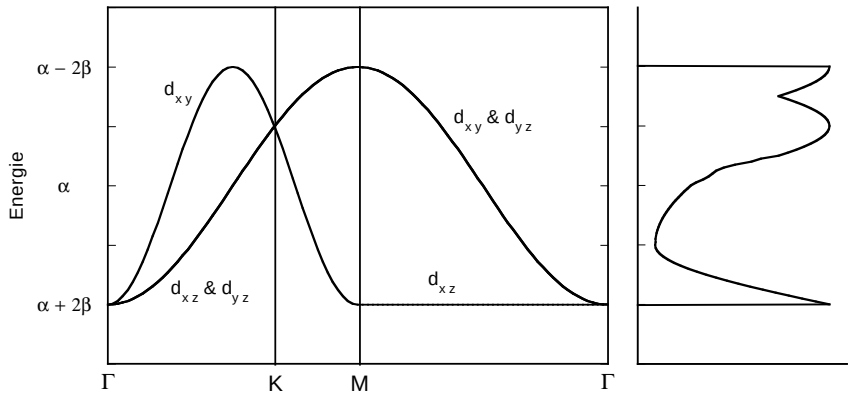

Figure 6. The dispersion of the band calculated by considering only σ-interaction between t_{2g} orbitals. The expected DOS is also shown.

It is interesting to note that a minimum of the density of states gives rise to a pseudo-gap just below the Fermi level. Let us comment on the origin of this pseudo-gap. It does not seem to be an artefact of the LMTO calculation since a similar feature is also observed in the band structures of TiS_2 and $LiTiS_2$ obtained from a LAPW calculation [16]. In fact it results from the hidden 1D structure of the VS_2 or TiS_2 layer. As shown by Whangbo and Canadell [17], these octahedral TS_2 layers (T = Ti, V, Cr) can be described as edge-sharing octahedral chains running along the direction $\boldsymbol{a}$, $\boldsymbol{b}$ or $\boldsymbol{a} + \boldsymbol{b}$ (figure 5(a)). The equatorial plane of each chain (which contains the shared edges of the TS_6 octahedra) is parallel to the (x, y), (x, z) or (y, z) plane where we use the directions pointing towards the ligands as the x-, y-, and z-axes. This plane contains one of the three t_{2g} orbitals, d_{xy}, d_{xz} or d_{yz}, respectively. As a consequence, the metal–metal interactions resulting from the in-plane t_{2g} orbitals are strong (σ-type) along each chain direction, but weak between adjacent chains (pseudo-δ-type). To a first approximation the t_{2g} band can thus be viewed as a superposition of three independent 1D bands. Assuming only a nearest-neighbour interaction, the dispersion of a 1D band within the LCAO scheme is given by $E(k) = \alpha + 2\beta\cos(ka)$ (α being the self-energy of an electron in the atomic orbital, β the interaction between nearest neighbours, a the lattice spacing). Starting from this well known formula, it is easy to calculate the dispersion of the three t_{2g} bands in the first Brillouin zone (FBZ) of the TS_2 layer shown in figure 5(b). This dispersion shown in figure 6 agrees qualitatively with the dispersion given by the LMTO calculation. This establishes the quasi-1D character of the t_{2g}–t_{2g} intralayer interactions. The orbital combinations leading to this dispersion can be described in the following way near the high-symmetry points of the FBZ. At the zone centre Γ, the three t_{2g} crystal orbitals are degenerate in the most bonding state ($E_\Gamma = \alpha + 2\beta$). But the degeneracy is lifted at point M. The k-vector at this point is perpendicular to the chain which contains the d_{xz} orbitals. The crystal orbital built from the d_{xz} orbitals remains in the most strongly bonding state while the crystal orbitals formed from the d_{xy} or d_{yz} orbitals are in the most strongly anti-bonding state ($E = \alpha - 2\beta$). At point K the three t_{2g} crystal orbitals are degenerate in an intermediate anti-bonding state ($E = \alpha - \beta$). These orbital combinations are shown in figure 7. As a consequence of this degeneracy lifting, the overall t_{2g} band is split into two subbands which can be viewed in the DOS of figure 6 and which reflect the results of the LMTO calculation (see figure 4(b)).

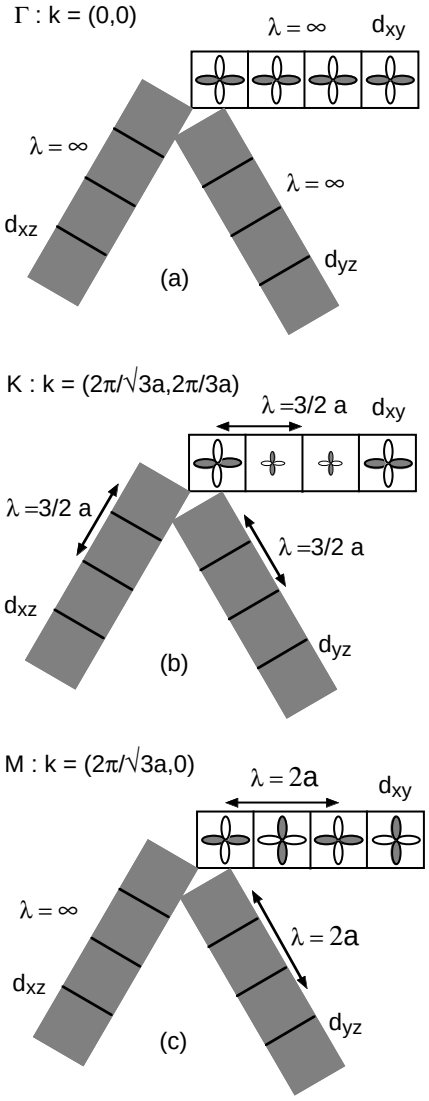

Figure 7. Orbital combinations in each chain at different k-points of the first Brillouin zone: Γ (0 0 0), K (−1/3 2/3 0), M (0 1/2 0).

4. Physical properties

The presence of a finite density of states at the Fermi level should lead to a metallic behaviour for '$LaVS_3$'. The electrical resistivity of different crystals from batch 1 has been measured within the standard four-probes configuration. Figure 8(a) gives the temperature dependence of the resistivity $\rho(T)$ between 2 K and 300 K: it is clear that this compound is non-metallic, as was also found by Kondo *et al* [7] and Nishikawa *et al* [8]. At low temperature ($T <$ 30 K), $\rho(T)$ follows an $\exp(T_0/T)^{1/2}$ law (cf. figure 8(b)). Above 30 K the temperature dependence changes to an $\exp(T_0/T)^{1/4}$ law. These dependences suggest that conduction takes place by hopping. Deviations from these laws are observed above 150 K. This leads

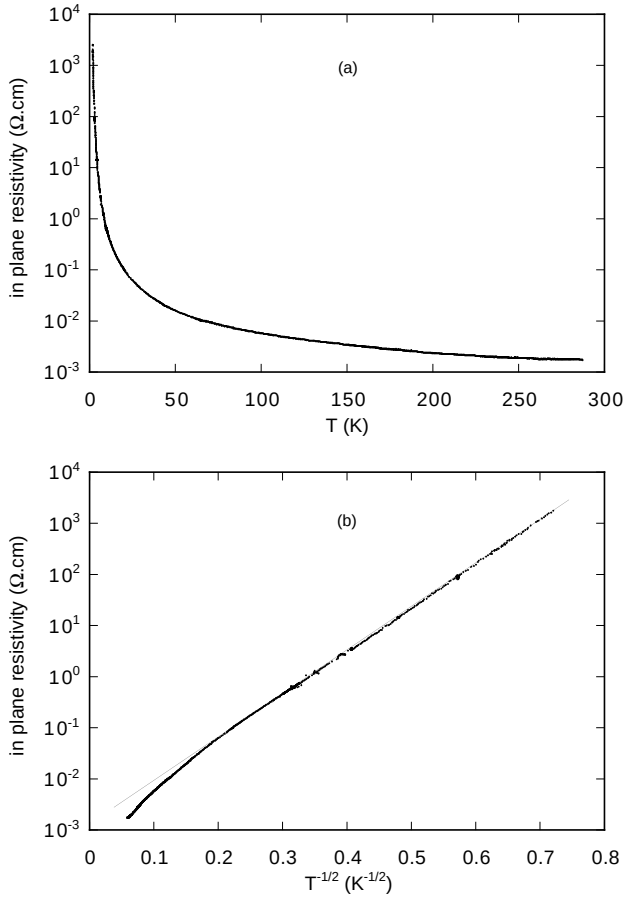

Figure 8. The 2 K–300 K temperature dependence of the resistivity of a stoichiometric single crystal of '$LaVS_3$' (a) versus T and (b) versus $T^{1/2}$.

to an activated behaviour above 300 K with an activation energy $E = 14.2$ meV. At room temperature the resistivity is close to 2 mΩ cm. This value is rather low and is comparable to Mott's minimum metallic conductivity. It is worth noting that measurements on four different crystals show a small dispersion of the room temperature resistivity (ranging from 1 to 3 mΩ cm) while the temperature dependence of the resistivity is unaffected. This dispersion exceeds the experimental uncertainties and may arise from the anisotropic character of the conductivity in the (a, b) plane resulting from the hidden 1D chains of the VS_2 layer discussed above. However, a small change in composition (due to a La vacancy) from one crystal to another cannot be excluded.

Conversely, the magnetic susceptibility measured with a SQUID susceptometer is Pauli-like in agreement with the results of [8]. A small Curie tail corresponding either to 1% of V^{3+} or to 3%/(V atom) of spin-1/2 paramagnetic impurities is observed below 50 K. The temperature-independent value of 4.6×10^{-4} emu mol^{-1} would correspond to a density of states at the Fermi level of 13.8 states eV^{-1}/(V atom), larger than expected from the DOS calculation (2.2 states eV^{-1}/(V atom)).

5. Discussion

In the preceding sections we have shown that, as expected from a rough estimate of the charge transfer, '$LaVS_3$' should be a metal (as should the Ti and Cr compounds of the series). Band-structure calculations confirm this fact and show that the VS_2 layer should be the active layer as regards the transport properties. However, the resistivity of '$LaVS_3$' single crystals clearly shows that this compound is non-metallic even if the magnetic susceptibility is temperature independent. One way to explain this apparent discrepancy is to suppose that the band-structure calculation according to the LMTO-ASA scheme is not valid here. However, note that the same kind of calculation for the Ti and Cr compounds shows that the Ti compound should also be metallic and it is, while the Cr compound should be an insulator and it is. Furthermore, a study of the comparison with $LiVS_2$ is instructive as regards this point.

The structure of this latter compound [18] can be deduced from the structure of the '$LaVS_3$' compound by replacing the LaS layer with intercalated Li atoms. Within the VS_2 layers of $LiVS_2$, the V–S distance (2.43 Å) is close to the average V–S distance observed in '$LaVS_3$' (2.40 Å). This means that the octahedra surrounding the V atoms are nearly identical for the two compounds and it suggests that this compound can be used as a model for '$LaVS_3$'. The results of the LMTO calculation for $LiVS_2$ (space group $P\bar{3}m1$) are shown in figure 9. The DOS is very similar to the DOS of the VS_2 part of '$LaVS_3$' as expected from the rigid-band consideration developed above. It can be described in the same way. The S 3s and also the S 3p bands are found at low energies while the V 3d bands are encountered close to the Fermi level. The t_{2g} band which also extends over 2 eV is filled by two electrons (spin up and spin down). Note that the pseudo-gap discussed above also appears in the t_{2g} band. In this $LiVS_2$ material, the charge transfer is only of 1 electron/V (to be compared to 1.2 electrons/V for '$LaVS_3$'). This results in a shift of the Fermi level towards lower energies, just at the minimum of the pseudo-gap. However, in sharp contrast with what happens for '$LaVS_3$', the finite DOS at the Fermi level agrees with the experimental metallic properties (both resistivity and susceptibility) reported for this compound [19].

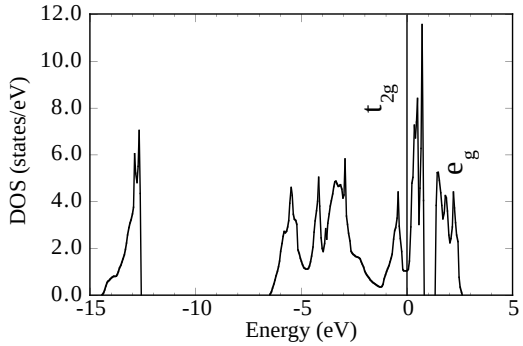

Figure 9. The DOS of $LiVS_2$ from the LMTO calculation.

At this stage, from LMTO calculations we have shown that '$LaVS_3$' and $LiVS_2$ should be metallic and that this behaviour should be mainly related to the VS_2 slab. However, only the latter compound is found to be metallic while the VS_2 slabs are exactly the same in the two compounds. One way to explain this discrepancy is to consider the validity of the LMTO calculation. We may ask whether this method has underestimated the gaps. As the Fermi level is located close to a minimum of the DOS, a true gap larger than the calculated pseudo-gap might lead to a semiconductor-like conduction. Indeed, this can explain the temperature

dependence of the resistivity of '$LaVS_3$' which is activated above room temperature. However, in $LiVS_2$ for which the Fermi level is closer to the minimum of the DOS than for '$LaVS_3$', the resistivity is metallic-like. Thus it is unlikely that the pseudo-gap is a true gap.

Other points which are not taken into account in the LMTO method are the correlation effects. We have experimental evidence that electronic correlations are present in these materials. For '$LaVS_3$' the low-temperature dependence ($T < 30$ K) of the resistivity, $\rho \propto \exp(T_0/T)^{1/2}$, is indicative of a hopping conduction in the presence of electronic correlations. Furthermore, the reported magnetic susceptibilities of $LiVS_2$ and '$LaVS_3$' are much stronger than expected from the density of states at the Fermi level. For example, the Pauli susceptibility of 4.6×10^{-4} emu mol^{-1} for '$LaVS_3$' corresponds to a density of states at the Fermi level of 13.8 states eV^{-1}/(V atom). This is much higher than the results of our calculation or the rough estimate of 3 states eV^{-1}/(V atom) that can be expected for a 2 eV wide t_{2g} band with a DOS of 6 states/(V atom). The magnetic susceptibilities are increased by Coulomb enhancement. It is well known that electronic correlations can lead to an insulator-like behaviour. Still, the $LiVS_2$ material is metallic while the '$LaVS_3$' compound is not. It is thus hard to believe that the electronic correlations alone can explain the difference in behaviour of the two compounds.

In fact, a structural difference between the two compounds has not been discussed so far. $LiVS_2$ has a commensurate structure while the structure of '$LaVS_3$' is incommensurate. In our calculation, we have used the simplest commensurate structure of '$LaVS_3$'. We have already remarked that this assumption leads to a very small contraction of the distances in the LaS layer and we still believe that this does not influence the results of our calculation very much. A more dramatic effect caused by the incommensurability is that in '$LaVS_3$' any atomic position is shifted from the average position by a displacive modulation. This modulation is actually absent in $LiVS_2$. It is not taken into consideration in our calculation. For the parent compound '$LaVSe_3$' [20] a precise structural analysis has shown that the largest amplitude of the displacive modulation is encountered at the V sites. In this compound, the distance between two V neighbours can be modulated over as much as 0.63 Å. If a modulation of same order of magnitude was present in '$LaVS_3$', it would lead to drastic differences in the overlap between the neighbouring t_{2g} orbitals. This kind of effect resembles the energy disorder leading to an Anderson localization. Once more, we do not believe that this is the case here, because the magnetic susceptibility of this material still shows signs of metallicity. In fact the modulation has a much longer wavelength than the lattice constant. It is more appropriate to think of an inhomogeneous VS_2 layer with regions in which the V–V distances are short, these regions being metallic, separated by regions (or links) in which the V–V distances are so long that they prevent an efficient transfer. In such a material, the states will be delocalized over sizable but finite lengths: this should lead to a metallic susceptibility; however, the dc conductivity will occur by hopping across the insulating region. Indeed, both electron correlations and strong modulation effects are responsible for the observed behaviour in '$LaVS_3$': a non-metallic conductivity but a metallic susceptibility.

This analysis together with our band structure explains as well the variation of the electronic properties as a function of the Sr substitution in '$LaVS_3$' described by Nishikawa *et al* [8]. They have reported that in the $(La_{1-x}Sr_xS)_{1.17}VS_2$ series a critical Sr content $x_c = 0.15$ exists above which the conduction changes from n-type to p-type. x_c is associated with a minimum of the heat capacity. Further increasing the Sr content leads to a metal–insulator transition at $x \approx 0.3$. Upon Sr substitution, the electronic transfer from the LaS to the VS_2 layer decreases. It shifts the Fermi level across the pseudo-gap from the electron-type region to the hole-type region. This is in agreement with the n-type and p-type conduction found for $x < x_c$ and $x > x_c$ respectively. Furthermore, the minimum of the heat capacity (which gives

a measure of the DOS at E_F) for $x = x_c$ and its increase apart from this value is consistent with the Fermi level crossing the minimum of the DOS found in our calculation. A further decreasing transfer will shift the Fermi level into a region where the states are fully delocalized, as observed for $x > x_c$.

6. Conclusions

In summary, the LMTO band-structure calculation of '$LaVS_3$' has shown three major features:

(a) The band structure can be derived from a rigid-band scheme using the structure of the LaS and of the VS_2 layers stabilized by the charge transfer.
(b) The states responsible for the electrical properties of this compound belong to the t_{2g}–e_g-split V 3d bands.
(c) A pseudo-gap opens in this band due to the intralayer bonding of the t_{2g} orbitals.

These results are not sufficient to explain the physical properties of this compound. We suggest that strong electron correlations together with a significant modulation of the V atomic position induced by the incommensurability have to be taken into account. In '$LaVS_3$', this leads to a segregation between metallic regions responsible for the Pauli-like susceptibility and insulating barriers which are responsible for a hopping mechanism of conductivity. In $LiVS_2$, there is no significant modulation. The material is a correlated metal. Changing the nature of the transition element on going to the Cr compounds, a contraction of the d orbital around the Cr ion leads to a less efficient screening of the electronic repulsion. The electronic correlations are enhanced. The material then behaves like a Mott insulator. On the other hand, in the Ti compounds the correlations are reduced. Furthermore, the modulation is smaller. The material then behaves as a metal. In all of these materials, there is a charge transfer of about one electron to the TS_2 layer. The incommensurability may play a key role as regards the physical properties when its effects are added to the electronic correlations.

Acknowledgments

We acknowledge F Boucher for help in performing the band-structure calculations and O Rouer for help in the microprobe analyses.

References

[1] Wiegers G A and Meerschaut A 1992 *Incommensurate Sandwiched Layered Compounds* ed A Meerschaut (Zurich: Trans Tech)
Wiegers G A and Meerschaut A 1992 *Mater. Sci. Forum* **100+101** 101
[2] Wiegers G A 1996 *Progress in Solid State Chemistry* vol 24 (Amsterdam: Elsevier) p 1
[3] Lafond A, Meerschaut A, Rouxel J, Tholence J L and Sulpice A 1995 *Phys. Rev.* B **52** 1112
[4] Rouxel J, Meerschaut A and Wiegers G A 1995 *J. Alloys Compounds* **229** 144
[5] Kondo T, Suzuki K and Enoki T 1995 *J. Phys. Soc. Japan* **64** 4296
[6] Cario L, Johrendt D, Lafond A, Felser C, Meerschaut A and Rouxel J 1997 *Phys. Rev.* B **55** 9409
Fang C M, de Groot R A, Wiegers G A and Haas C 1997 *J. Phys. Chem. Solids* **58** 1103
[7] Kondo T, Suzuki K and Enoki T 1992 *Solid State Commun.* **84** 999
Suzuki K, Kendo T, Enoki T and Bandow S 1993 *Synth. Met.* **55–57** 1741
[8] Nishikawa T, Yasui Y and Sato M 1994 *J. Phys. Soc. Japan* **63** 3218
Yasui Y, Nishikawa T, Kobayashi Y, Sato M, Nishioka T and Kontani M 1995 *J. Phys. Soc. Japan* **64** 3890
Nishikawa T, Yasui Y, Kobayashi Y and Sato M 1996 *Physica* C **263** 554
[9] Moelo Y, unpublished results
[10] Rouxel J, Moelo Y, Lafond A, DiSalvo F J, Meerschaut A and Roesky R 1994 *Inorg. Chem.* **33** 3358

[11] Kato K, Onoda M, Sato A, Cho N W, Kikkawa S, Kanamaru F, Ohsumi K, Takase T, Uchida M, Jarchow O and Friese K 1995 *Z. Kristallogr.* **210** 432
[12] Kikkawa S, Nakatuka A, Cho N W and Kanamaru F 1995 *Eur. J. Solid State Inorg. Chem.* **32** 771
[13] Cario L, Meerschaut A, Moelo Y, Nader A and Rouxel J 1997 *Eur. J. Solid State Inorg. Chem.* **34** 913
[14] Andersen O K and Jepsen O 1984 *Phys. Rev. Lett.* **53** 2571
Krier G, Jepsen O, Burkhardt A and Andersen O K (ed) 1994 *TB-LMTO-ASA 47 Program: a Program for ab initio Band Calculations* (Stuttgart: Max-Planck-Institut)
[15] Lambrecht W R and Andersen O K 1986 *Phys. Rev.* B **34** 2439
[16] Umrigar C, Ellis D E, Wang Ding-sheng, Krakauer H and Posternak M 1982 *Phys. Rev.* B **26** 4935
[17] Whangbo M H and Canadell E 1992 *J. Am. Chem. Soc.* **114** 9587
[18] van Laar B and Ijdo D J W 1971 *J. Solid State Chem.* **3** 590
[19] This calculation explains also the metallic-like character reported for the Li_xVS_2 and Na_xVS_2 (Na at trigonal sites) series ($x < 1$); see, for example,
Murphy D W, Cros C, Di Salvo F J and Waszczak J V 1977 *Inorg. Chem.* **16** 3027
van Bruggen C F, Haas C and Wiegers G A 1979 *J. Solid State Chem.* **27** 9
[20] Ren Y, Baas J, Meetsma A, de Boer J L and Wiegers G A 1996 *Acta Crystallogr.* B **52** 398